J Electr Eng Technol.2015;10(1): 271-279
http://dx.doi.org/10.5370/JEET.2015.10.1.271

ISSN(Print) 1975-0102
ISSN(Online) 2093-7423

Buck-Boost Interleaved Inverter Configuration for Multiple-Load Induction Cooking Application

Sharath Kumar. P†, Vishwanathan. N* and Bhagwan K. Murthy*

Abstract – Induction cooking application with multiple loads need high power inverters and appropriate control techniques. This paper proposes an inverter configuration with buck-boost converter for multiple load induction cooking application with independent control of each load. It uses one half-bridge for each load. For a given dc supply of V_{DC}, one more V_{DC} is derived using buck-boost converter giving $2V_{DC}$ as the input to each half-bridge inverter. Series resonant loads are connected between the centre point of 2 V_{DC} and each half-bridge. The output voltage across each load is like that of a full-bridge inverter. In the proposed configuration, half of the output power is supplied to each load directly from the source and remaining half of the output power is supplied to each load through buck-boost converter. With buck-boost converter, each half-bridge inverter output power is increased to a full-bridge inverter output power level. Each half-bridge is operated with constant and same switching frequency with asymmetrical duty cycle (ADC) control technique. By ADC, output power of each load is independently controlled. This configuration also offers reduced component count. The proposed inverter configuration is simulated and experimentally verified with two loads. Simulation and experimental results are in good agreement. This configuration can be extended to multiple loads.

Keywords: Series resonant inverter, Buck-boost converter, Induction heating, Asymmetrical duty cycle control

1. Introduction

Induction cooking is one of the several applications of induction heating. Induction heating method is a far better approach than other conventional methods. In conventional methods, the heat is transferred from heat source to load by conduction or radiation. In induction heating, the heat is developed inside the load due to generation of eddy currents at skin depth level from the surface [1]. In recent times, considerable progress is made in control schemes and inverter configurations. A typical arrangement of high frequency (HF) induction heating circuit is shown in Fig. 1.

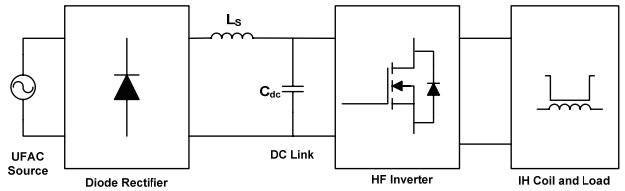

Fig. 1. Typical arrangement of high frequency induction heating resonant inverter

Resonant inverter is commonly used as a source of high frequency AC supply. The DC input to it is derived by rectifying the utility AC source. High frequency AC flowing in the load coil results in eddy currents induced in the vessel at skin depth level resulting in heating effect. The eddy currents produced in the load are concentrated in a peripheral layer at skin depth (δ), which is expressed as

$$\delta = \sqrt{\frac{\rho}{\pi \mu f_s}} = \sqrt{\frac{1}{4\pi^2 \times 10^{-7}}} \times \sqrt{\frac{\rho}{\mu_r f_s}} \quad (1)$$

where, ρ is electrical resistivity, μ is magnetic permeability, μ_r is relative magnetic permeability of the load material, and f_s is switching frequency of the inverter. Commonly used topologies for induction cooking application are quasi resonant, half-bridge, and full bridge inverters [2-4]. Out of these, full bridge inverter is preferred for high power applications. Half-bridge inverter is preferred for less components count. Multiple-load half-bridge series resonant inverter is shown in Fig. 2.

In this, L_{r1} is the coil inductance, C_{r1} is the resonant capacitance, and R_{eq1} is equivalent resistance of the load-1. Similarly, L_{r2}, C_{r2}, and R_{eq2} are the coil inductance, resonant capacitance, and equivalent resistance of the load-2 respectively. C_1 and C_2 are DC link split capacitors. Q_1 and Q_2 are the switching devices with anti-parallel diodes D_1 and D_2 of load-1 inverter circuit. Q_3 and Q_4 are the

† Corresponding Author: Dept. of Electrical Engineering, National Institute of Technology Warangal, India. (sharathpapani@nitw.ac.in)
* Dept. of Electrical Engineering, National Institute of Technology Warangal, India.
Received: June 22, 2014; Accepted: September 24, 2014

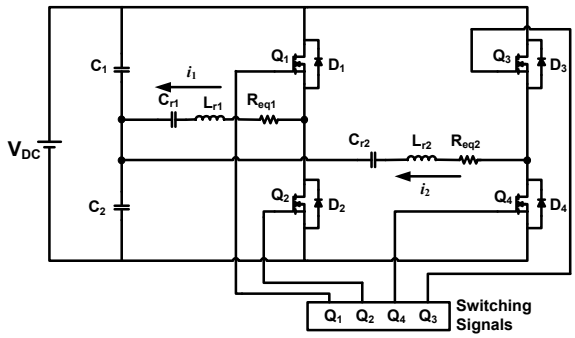

Fig. 2. Multiple-load half-bridge series resonant inverter

switching devices with anti-parallel diodes D_3 and D_4 of load-2 inverter circuit. V_{DC} is the supply voltage, i_1 is the load-1 resonant tank current and i_2 is the load-2 resonant tank current.

Pulse amplitude modulation (PAM) and pulse frequency modulation (PFM) were used to control output power in induction heating application. Under PAM control, amplitude of the source voltage is varied to control the output power [5]. It requires power processing at two stages i.e., one at AC to DC power conversion and other at high frequency inverter, resulting in more complexity and reduced efficiency. Under PFM control, the switching frequency has to be varied over a wide range [6]. Also, the soft switching operating region for zero voltage switching (ZVS) operation is relatively narrow. If the circuit operates below the resonance, the filter components are large at low frequency range. In [7], for induction heating application, phase shift control (PSC) technique is used for output power control. ZVS problem is minimized by varying the switching frequency. In [8], phase-shifted PWM and load-adaptive PFM control strategies are used. In [9], hybrid power control technique with pulse density modulation (PDM) and phase-shift modulation (PSM) are proposed for induction heating applications. These methods improve the performance of the inverter in several aspects. ZVS problem is also minimized by techniques such as asymmetrical voltage cancellation (AVC) and asymmetrical duty cycle (ADC) control [10]. In [11], two operating modes for power control of half-bridge resonant inverter induction heating system are described. One operating mode uses variable frequency control for larger output power. Other operating mode uses pulse density modulation control in low to medium power range. It has the advantage of high efficiency over wide output power range. The limitation is the use of variable frequency control in certain power range.

In induction cooking application, one inverter feeds power to a single load. For multiple load application, there is a need to develop inverter circuits and control techniques which can minimize components count and provide independent control of each load. Certain techniques are available in the literature. In [12], single inverter with two load system is proposed and analyzed. It uses variable switching frequency control. This scheme has one master load and one slave load. It has several resonant capacitors connected in parallel by electro-mechanical switches. These are activated for power control. In [13], an inverter configuration for two loads is suggested. It has three legs wherein one leg is common for both the loads. This configuration provides independent and simultaneous control of both loads. Asymmetric voltage cancellation technique is used for control of the inverters. This method has the advantage of reduced components count and better utilization of devices. This technique can be extended to more than two loads also. In [14], two-output charge boost type induction cooking application is proposed using asymmetrical voltage cancellation technique. A power factor correction stage is also added to improve the power factor. In [15], a load-adaptive control algorithm for variable load and large output power range is proposed and described. In the design process, aspects like efficiency, acoustic noise, and flicker emissions are considered. It is shown that single control strategy is not suitable when several aspects are to be considered. An appropriate combination of different control techniques is suggested for each power range. The limitation of this method is increased complexity in the control implementation. In [16], a cost-effective multiple-load system is proposed. It uses discontinuous mode control to improve light-load performance. Converter efficiency is increased by reducing switching frequency while maintaining proper power factor. Switching frequency range is between 20 to 150 kHz. Variable switching frequency is the limitation of this method. In [17], system-on-programmable chip and FPGA based test bench for multiple inductor power converter is proposed. The power converter is modelled in VHDL. This speeds-up the simulation process of the system. In [18], multiple output induction heating system which uses direct ac-ac power conversion is proposed. This method gives higher efficiency, reduced components count and reduced complexity. This is achieved with the use of matrix converter for multiple loads. Variable frequency control may be the limitation of this method. Also, larger input harmonic currents are present under unbalanced operation.

This paper proposes buck-boost interleaved inverter configuration for induction cooking application with multiple-loads. It uses one half-bridge for each load. For a given dc supply of V_{DC} one more V_{DC} is derived using buck-boost converter giving $2V_{DC}$ as the input to each half-bridge. Series resonant loads are connected between the centre point of $2V_{DC}$ and each half-bridge. Output voltage is switched between $+V_{DC}$ and $-V_{DC}$ with half-bridge configuration. In the proposed configuration, half of the output power is supplied to each load directly from the source and remaining half of the output power is supplied to each load through buck-boost converter. With buck-boost converter, each half-bridge inverter output power is increased to a full-bridge inverter output power level. Each half-bridge is operated with constant and same switching

frequency with ADC control technique. By ADC [9], output power of each load is independently controlled. The proposed configuration can be extended to multiple-loads.

2. Proposed Inverter Configuration

This section describes the proposed inverter configuration for multiple-load induction cooking application. Circuit diagram of the proposed inverter is shown in Fig. 3 for two loads. Both loads use series resonant circuit. It uses one half-bridge for each load. For a given dc supply of V_{DC} one more V_{DC} is derived using buck-boost converter giving $2V_{DC}$ as the input to each half-bridge. Due to polarity reversing nature of output voltage in buck-boost converter, it becomes possible to use input and output voltages of buck-boost converter as two dc sources like split capacitor configuration of half-bridge inverter. With suitable duty ratio of buck-boost converter, it is possible to maintain output voltage equal to input voltage (V_{DC}) for all induction heating loads. Hence, input and output voltages of buck-boost converter are maintained at equal magnitude. This gives total input voltage of $2V_{DC}$ to each half-bridge inverter, which is also a series connection of two dc sources each of V_{DC}. The buck-boost converter is switched at 30 kHz.

Series resonant loads are connected between the centre point of $2V_{DC}$ and each half-bridge as shown in Fig. 3. The output voltage across each load switches between $+V_{DC}$ and $-V_{DC}$ with half-bridge configuration. It is similar to that of a full bridge inverter with V_{DC} as the DC input. Hence in this proposed configuration, each load handles same power as that supplied from a full-bridge configuration. Each half-bridge is operated with constant and same switching frequency with ADC control technique. By ADC, output power of each load is independently controlled. Load-1 is connected to inverter output voltage v_{AB}. Load-2 is connected to inverter output voltage v_{AC}. Load-1 consists of C_{r1}, L_{r1}, and R_{eq1} which are resonant capacitance, inductance and equivalent load resistance respectively making series resonant tank. Similarly, load-2 consists of C_{r2}, L_{r2}, and R_{eq2}, which are resonant capacitance, inductance and equivalent load resistance respectively making series resonant tank. Resonant frequencies of two load circuits are $f_{r1} = \frac{1}{2\pi\sqrt{L_{r1}C_{r1}}}$ and $f_{r2} = \frac{1}{2\pi\sqrt{L_{r2}C_{r2}}}$ respectively. If required they can be of different power ratings, but operated at same switching frequency. Hence, the resonant frequencies of both load circuits have to be same.

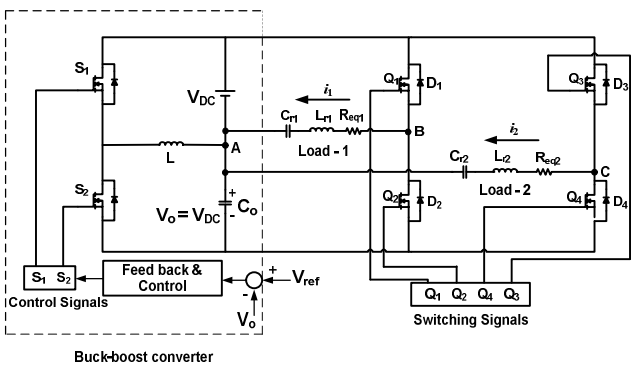

Fig. 3. Proposed inverter configuration for multiple-load induction cooking

In this paper, both loads have same component values and their resonant frequencies are same. $L_{r1} = L_{r2} = L_r$, $C_{r1} = C_{r2} = C_r$, and $R_{eq1} = R_{eq2} = R_{eq}$. Hence, their power rating is same and operated at a switching frequency of 30 kHz. Resonant frequency of each load circuit is, $f_r = \frac{1}{2\pi\sqrt{L_rC_r}}$.

Switching frequency of each leg is slightly higher than their resonant frequency. Hence, inverter switching frequency (f_s) can be chosen 5 to 10% higher than the resonant frequency (f_r) for ZVS operation.

Fig. 4 shows gating signals v_{g1} and v_{g2} for the switching devices Q_1 and Q_2 of half-bridge inverter for load-1. Also, output voltage (v_{AB}) along with its fundamental component (v_{AB1}) is shown. The load-1 current (i_1) is shown assuming it to be sine wave due to filtering of harmonics by resonant load. These waveforms are based on ADC control technique. Here, the angles θ_1 or β_1 can be used as control variables and $\beta_1 = (180° - \theta_1)$. $\varnothing_1$ is the angle between v_{AB1} and i_1. β_1 can be controlled to control the duty-ratio of output voltage (v_{AB}). The duty-ratio (D_1) of load-1 half-bridge inverter is defined as

$$\text{Duty ratio } (D_1) = \frac{T_{on}}{T/2} \tag{2}$$

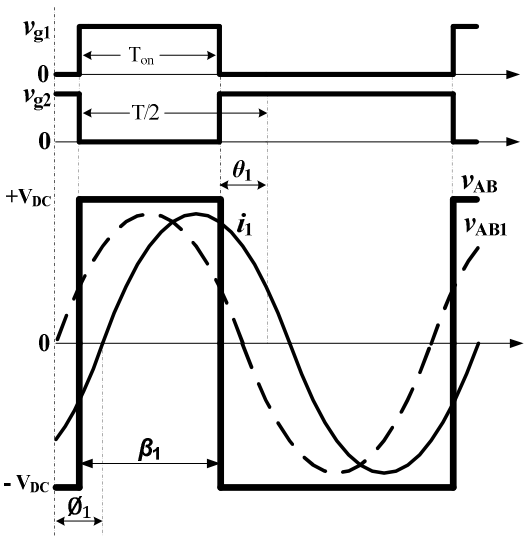

Fig. 4. Output voltage and current with control variables with ADC control technique

In Fig. 4, T_{on} and T/2 are shown with gating pulses for load-1 half-bridge inverter. Analysis of asymmetrical duty cycle control for series resonant inverter is presented in [10]. Harmonics in load current waveform are negligibly small and ignored.

The amplitude of the fundamental voltage $\hat{v}_{AB1}$ can be expressed in ADC control technique as,

$$\hat{v}_{AB1} = \frac{4V_{dc}}{\pi}\cos\frac{\theta_1}{2} \tag{3}$$

$\hat{I}_1$ is the amplitude of the load-1 current and assumed to be sinusoidal. The phase lag $\varnothing_1$ between the voltage v_{AB1} and the load current i_1 can be expressed as,

$$\varnothing_1 = \tan^{-1}\left(\frac{\omega_s L_r - \frac{1}{\omega_s C_r}}{R_{eq}}\right) = \tan^{-1}\left(Q\left(\omega_n - \frac{1}{\omega_n}\right)\right) \tag{4}$$

The quality factor (Q) and normalized switching frequency (ω_n) are defined as

$$Q = \frac{\sqrt{\frac{L_r}{C_r}}}{R_{eq}} \tag{5}$$

$$\omega_n = \frac{\omega_s}{\omega_r} \quad \text{and} \quad \omega_r = \frac{1}{\sqrt{L_r C_r}} \tag{6}$$

where ω_s is angular switching frequency and ω_r is angular resonant frequency.

The resonant tank circuit current ($\hat{I}_1$) is expressed as,

$$\text{Where} \quad \hat{I}_1 = \frac{\hat{v}_{AB1}}{|Z_{eq}|} = \frac{4V_{DC}}{\pi|Z_{eq}|}\cos\frac{\theta_1}{2} = \frac{4V_{DC}\cos\varnothing}{\pi R_{eq}}\cos\frac{\theta_1}{2} \tag{7}$$

where $\varnothing = \varnothing_1$

The load-1 output power can be expressed as,

$$P_{o1} = \frac{\hat{I}_1^2}{2}R_{eq1}$$

$$P_{o1} = \frac{8V_{DC}^2\cos^2\varnothing}{\pi^2 R_{eq1}}\cos^2\frac{\theta_1}{2} \tag{8}$$

$$\text{Similarly,} \quad P_{o2} = \frac{8V_{DC}^2\cos^2\varnothing}{\pi^2 R_{eq2}}\cos^2\frac{\theta_2}{2} \tag{9}$$

where P_{o2} is output power of load-2 and θ_2 is control variable for load-2. The total output power (P_T) is expressed as $P_T = P_{o1} + P_{o2}$. From the above equations, the amplitude of individual currents and output powers can be controlled by varying corresponding control angles θ_1 and θ_2. As θ_1 and θ_2 can be independently controlled, both loads are independently controllable.

The output voltage across each load is like that of a full-bridge inverter. Hence the output power increases with proposed configuration. In the proposed configuration, half of the output power is supplied to each load directly from the source and remaining half of the output power is supplied to each load through buck-boost converter.

The buck-boost converter shown in Fig. 3 needs to be controlled in closed loop to maintain its output voltage equal to input voltage under different load conditions. Since, half of the load power is processed through buck-boost converter, losses in buck-boost converter have to be minimized as much as possible. This helps in improving overall efficiency of the proposed configuration. For this, in place of free-wheeling diode power MOSFET (S_2) is used. This reduces losses during free-wheeling. Also, both MOSFETs used in buck-boost converter are of low on-state resistance.

For, P_{in} = inverter input, and P_T = total inverter output

η_I = inverter efficiency = $\frac{P_T}{P_{in}}$

η_B = efficiency of buck-boost converter

η = overall efficiency (with buck-boost converter)

$$= \frac{P_T}{\left[\frac{P_{in}}{2} + \frac{P_{in}}{2\eta_B}\right]} = \frac{\eta_I}{\left[0.5 + \frac{0.5}{\eta_B}\right]} \tag{10}$$

Overall efficiency is dependent on η_B. For ideal buck-boost converter, $\eta_B = 1$ and $\eta = \eta_I$. Under practical condition, η_B is less than unity. This results in $\eta < \eta_I$.

3. Results of Proposed Inverter Configuration

Experimental setup of proposed inverter configuration is shown in Fig. 5.

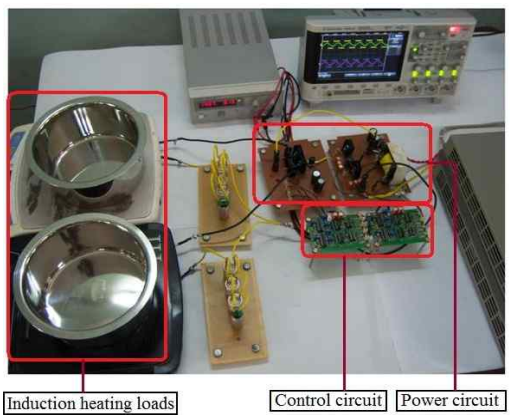

Fig. 5. Experimental setup of proposed inverter configuration

Table 1. Parameters of proposed inverter configuration for induction cooking

Item	Symbol	Value
Source voltage	V_{DC}	15V
Equivalent resistance of each load	R_{eq1}, R_{eq2}	1.95Ω
Equivalent inductance of each load	L_{r1}, L_{r2}	68μH
Resonant capacitance of each load	C_{r1}, C_{r2}	0.45μF
Resonant frequency of load circuit	f_r	28.77 kHz
Switching frequency of each leg	f_s	30 kHz
Dead time	t_d	450 nsec
MOSFETs used	IRFP4110PbF	100V, 180A

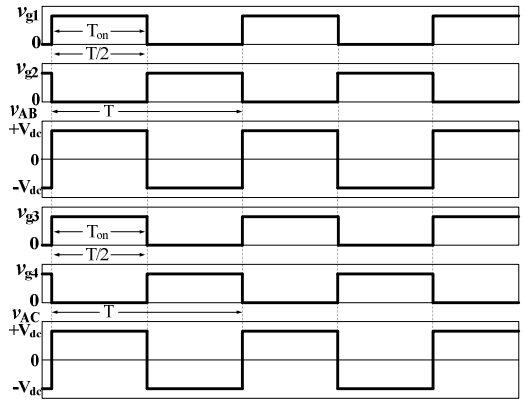

(a) Inverter gate pulses and output voltages (v_{AB} and v_{AC})

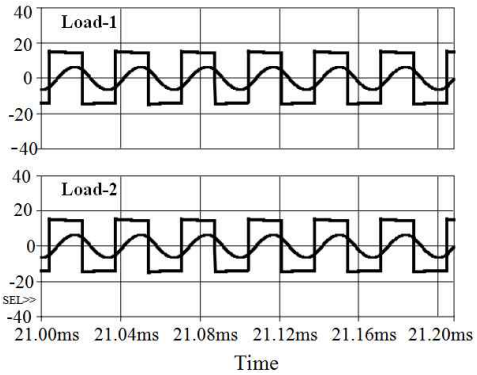

(b) Simulation waveforms of v_{AB} and v_{AC} and i_1 and i_2

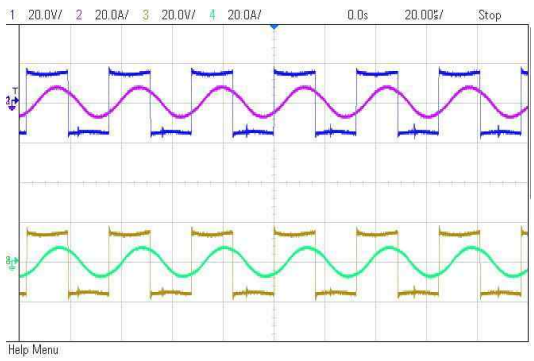

(c) Experimental waveforms of v_{AB} and v_{AC} and i_1 and i_2 (Scale: voltage: 20V/div., current: 20A/div.)

Fig. 6. Inverter waveforms for D_1= 0.97 and D_2= 0.97

Proposed inverter configuration with ADC control technique is simulated and experimentally verified using the parameters shown in Table 1.

Proposed circuit of half-bridge series resonant inverter configuration for two load induction cooking application is designed and operated at a switching frequency of 30 kHz. It is for a total output power (P_T) of 135 watts with a source voltage of 15V. The simulation and experimental studies are done for different duty-ratio combinations of D_1 and D_2. D_1 and D_2 are duty-ratios of inverter output voltages v_{AB} and v_{AC} respectively. Gate pulses, inverter output voltage

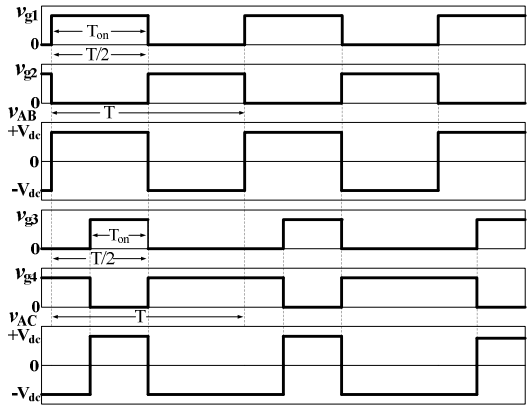

(a) Inverter gate pulses and output voltages (v_{AB} and v_{AC})

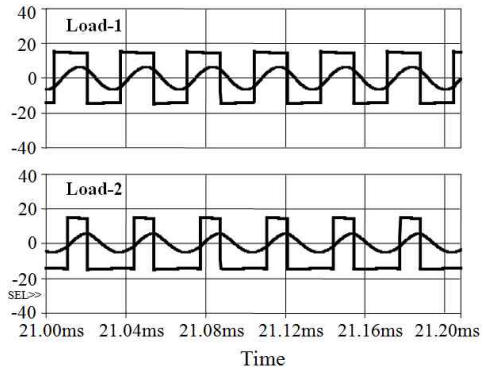

(b) Simulation waveforms of v_{AB} and v_{AC} and i_1 and i_2

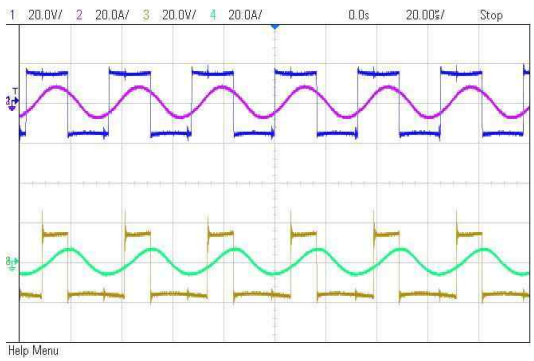

(c) Experimental waveforms of v_{AB} and v_{AC} and i_1 and i_2 (Scale: voltage: 20V/div., current: 20A/div.)

Fig. 7. Inverter waveforms for D_1= 0.97 and D_2= 0.6

waveforms and load currents for the proposed inverter configuration are shown in Figs. 6 to 9 for various duty-ratio combinations.

Figs. 6(a), 7(a), 8(a), and 9(a) show gate pulses v_{g1} to v_{g4} of switching devices Q_1 to Q_4 for various duty-ratio combinations of D_1 and D_2. These figures also show inverter output voltages v_{AB} and v_{AC} for these duty-ratio combinations. Fig. 6(a) shows these waveforms for D_1= 0.97 and D_2= 0.97. Figs. 7(a), 8(a), and 9(a) show them for D_1= 0.97 and D_2= 0.6, D_1= 0.7 and D_2=0.3, and D_1=0.5 and D_2=0.3 respectively. These figures help in understanding the operation of the proposed inverter configuration. Fig. 6(b) shows the simulation waveforms of both inverter output voltages and their load currents for a duty-ratio of D_1= 0.97 and D_2= 0.97.

Figs. 7(b), 8(b), and 9(b) show them for D_1= 0.97 and D_2= 0.6, D_1= 0.7 and D_2= 0.3, and D_1= 0.5 and D_2= 0.3 respectively. Similarly, Fig. 6(c) shows these waveforms of inverter output voltages and their load currents under experimental condition. In Fig. 6(c), D_1= 0.97 and D_2= 0.97. Figs. 7(c), 8(c), and 9(c) show them for D_1 = 0.97 and D_2 = 0.6, D_1 = 0.7 and D_2=0.3, and D_1 = 0.5 and D_2 = 0.3

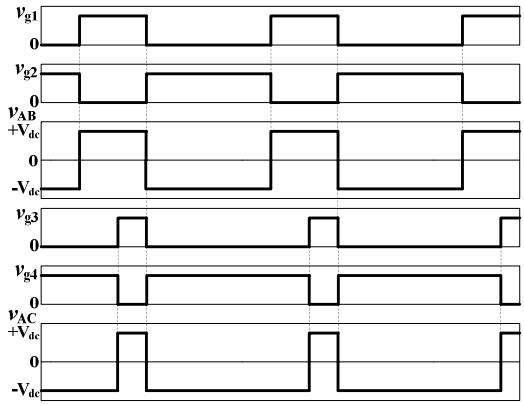

(a) Inverter gate pulses and output voltages (v_{AB} and v_{AC})

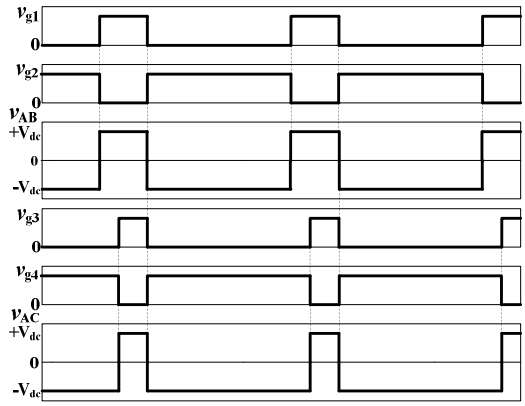

(a) Inverter gate pulses and output voltages (v_{AB} and v_{AC})

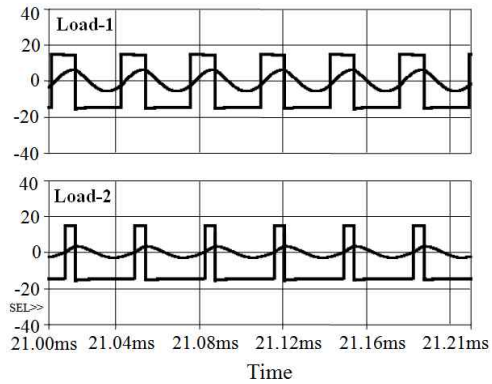

(b) Simulation waveforms of v_{AB} and v_{AC} and i_1 and i_2

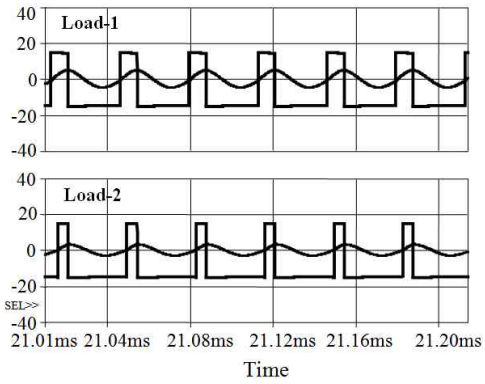

(b) Simulation waveforms of v_{AB} and v_{AC} and i_1 and i_2

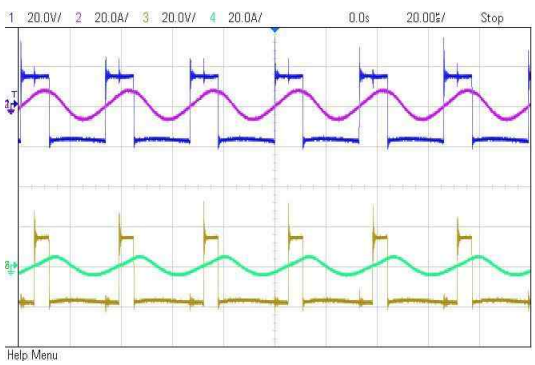

(c) Experimental waveforms of v_{AB} and v_{AC} and i_1 and i_2 (Scale: voltage: 20V/div., current: 20A/div.)

Fig. 8. Inverter waveforms for D_1= 0.7 and D_2= 0.3

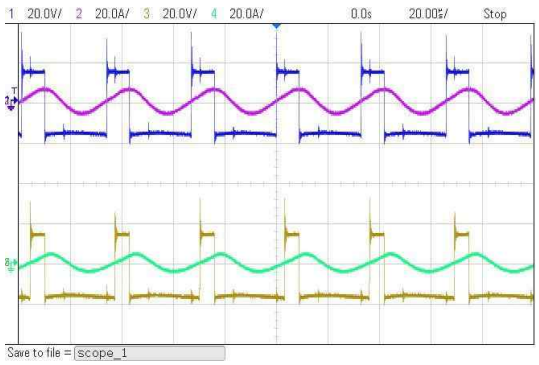

(c) Experimental waveforms of v_{AB} and v_{AC} and i_1 and i_2 (Scale: voltage: 20V/div., current: 20A/div.)

Fig. 9. Inverter waveforms for D_1= 0.5 and D_2= 0.3

respectively.

From Figs. 6 to 9, it can be observed that each output voltage waveform and its load current is independently controlled with ADC control technique. Independent control is achieved by variation of duty-ratios of individual inverters. This gives power control in each load independently.

From simulation and experimental results, it is observed that both results are in good agreement with each other. It is also seen that for a given DC input voltage of V_{DC}, the proposed inverter configuration of half-bridge series resonant inverter has same output voltage level as full-bridge configuration. This concept can be extended for multiple-loads also. Here, all loads can be operated at same switching frequency. In Figs. 6 and 7, duty-ratio of load-2 is 0.97 and 0.6 respectively, whereas duty-ratio of load-1 is kept constant at 0.97. It can be observed that current in load-2 varies with the variation of its duty-ratio, while the current in load-1 remains constant. Hence, current in load-2 is controlled independently. Similarly, in Figs. 8 and 9, duty-ratio of load-1 is 0.7 and 0.5 respectively, whereas duty-ratio of load-2 is kept constant at 0.3. It can be observed that current in load-1 varies with variation of its duty-ratio while the current in load-2 remains constant. Hence, current in load-1 is controlled independently. Proposed inverter configuration gives advantage of independent power control of each load. Though each load is powered with half-bridge configuration, it has output power capability of full-bridge. Also, it reduces component count for multiple loads.

In this paper, the switching frequency used for inverters is 30 kHz. Hence, ZVS is not of much concern. If required, the inverters can be switched at higher frequencies with possibility of ZVS.

4. Independent Control of Load Power

Load power control is achieved using ADC control technique. Output powers of load-1 and load-2 are dependent on corresponding load currents. In Table 2, load-1 current is controlled with its duty-ratio, and load-2 current remains constant as D_2 is kept constant at 0.97.

Similarly, it can be shown that when load-2 current varies with its duty-ratio and load-1 current remains constant. Each load current is controlled independently with its duty-ratio. It can be observed from Figs. 10 and 11.

Table 2. Load-1 current with its duty-ratio

Duty	Load-1	Load-1	Load-2	Load-2
0.97	5.99	5.9	5.99	5.9
0.9	5.81	5.76	5.99	5.9
0.8	5.62	5.58	5.99	5.9
0.7	5.16	5.09	5.99	5.9
0.6	4.71	4.68	5.99	5.9
0.5	4.23	4.15	5.99	5.9
0.4	3.57	3.44	5.99	5.9
0.3	2.76	2.6	5.99	5.9
0.2	1.89	1.9	5.99	5.9
0.1	0.98	0.99	5.99	5.9

Variation of current in load-1 with variation of D_1 is shown in Fig. 10. For this, D_2 is kept constant at 0.97. Under this condition, current in load-1 only varies whereas current in load-2 remains constant. Similarly, variation of current in load-2 with variation of D_2 is shown in Fig. 11. For this, D_1 is kept constant at 0.97. Under this condition, current in load-2 only varies whereas current in load-1 remains constant. Simulation and experimental results are in good agreement with each other.

In Fig. 12, variation of output power of load-1 vs. D_1 is shown with proposed configuration and with conventional half-bridge configuration. In the proposed configuration, output power is 4 times compared to conventional half-bridge configuration.

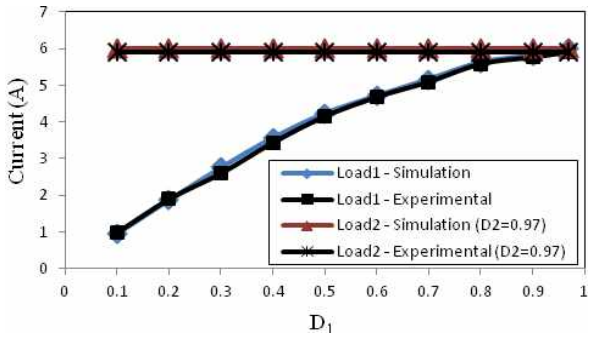

Fig. 10. Variation of current in load-1 vs. D_1

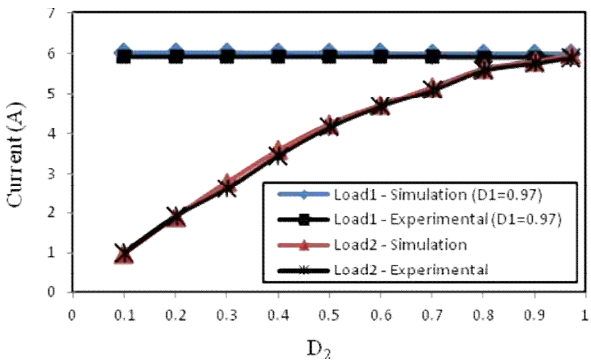

Fig. 11. Variation of current in load-2 vs. D_2

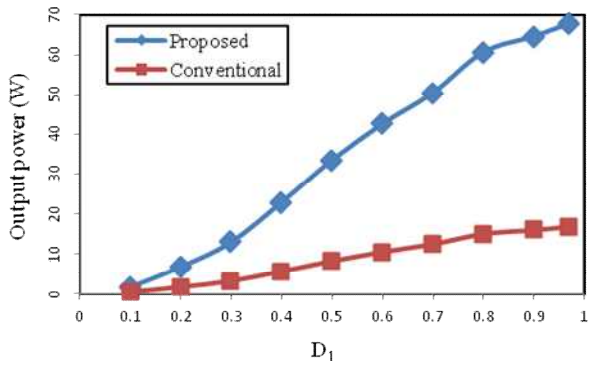

Fig. 12. Variation of output power for load-1 vs. D_1

5. Overall Efficiency

Overall efficiency for the proposed configuration is shown in Fig. 13. In Fig. 13, output power of load-1 is controlled while that of load-2 is kept constant at its maximum. Total output power is measured by addition of individual inverter outputs. Each inverter output is computed as I^2R_{eq}. 'I' is the r.m.s current value of individual load circuit. 'R_{eq}' is the equivalent load resistance of each load. Input power is obtained by multiplication of dc input voltage (V_{DC}) and average current of the source. Overall efficiency includes the efficiency of buck-boost converter also. To maintain high overall efficiency, buck-boost converter also should have high efficiency. It should be taken care in design stage.

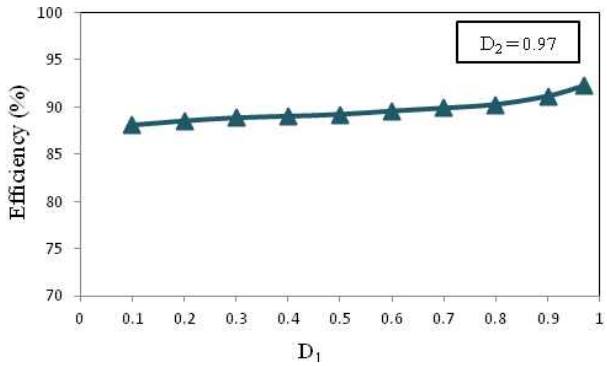

Fig. 13. Overall efficiency vs. D_1

Both of the loads are of same power capacity. Hence, overall efficiency characteristic will be same if output power of load-1 is kept constant and that of load-2 is varied. Under full-load condition, overall efficiency is > 93%.

6. Conclusions

In this paper, buck-boost interleaved inverter configuration with half-bridge series resonant inverters for two-load induction cooking application has been proposed. In this configuration, each half-bridge inverter output power is increased to a full-bridge inverter output power level. Both loads are independently controlled. It can be extended for more than two loads also. Excluding buck-boost converter, number of switching devices/load is two i.e., one leg/load. Same switching frequency is used for powering both the loads. i.e., each load is operated at same switching frequency of 30 kHz. Asymmetric duty cycle control technique is used for power control of individual loads. Under full-load condition, overall efficiency is >93%. Design and control of the proposed configuration are simple. Simulation and experimental results of the proposed configuration are in good agreement.

References

[1] W. C. Moreland, "The induction range: Its performance and its development problems," *IEEE Trans. Industry Applications*, vol. IA-9, no. 1, 1973, pp. 81-85.

[2] Masaki Miyamae, Takahiro Ito, Kouki Matsuse, Masayoshi Tsukahara, "Performance of a High Frequency Quasi-Resonant Inverter with Variable-Frequency Output for Induction Heating", *IEEE 7th International Power Electronics and Motion Control Conference*, Harbin, China, 2012.

[3] Mokhtar Kamli, Shigehiro Yamamoto, and Minoru Abe, "A 50-150 kHz Half-Bridge Inverter for Induction Heating Applications," *IEEE Trans. Industrial Electronics*, vol. 43, no.1, 1996, pp. 163-172.

[4] S.M.W. Ahmed, M.M. Eissa, M. Edress, T.S. Abdel-Hameed, "Experimental investigation of full-bridge Series Resonant Inverters for Induction-Heating Cooking Appliances", *4th IEEE Conference on Industrial Electronics and Applications*, ICIEA 2009, pp.3327-3332.

[5] Atsushi Okuno, Hitoshi Kawano, Junming Sun, Manabu Kurokawa, Akira Kojina, Mutsuo Nakaoka, "Feasible Development of Soft-Switched SIT Inverter with Load-Adaptive Frequency Tracking Control Scheme for Induction Heating," *IEEE Trans. Industry Applications*, vol. 34, no. 4, 1998, pp. 713-718.

[6] Young-Sup Kwon, Sang-Bong Yoo, Dong-Seok Hyun, "Half-Bridge Series Resonant Inverter for Induction Heating Applications with Load-Adaptive PFM Control Strategy", *14th Applied Power Electronics Conference and Exposition*, APEC' 99, vol. 1, 1999, pp. 575-581.

[7] L. Grajales, J. A. Sabate, K. R. Wang, W. A. Tabisz, F. C. Lee, "Design of a 10 kW, 500 kHz Phase-Shift Controlled Series-Resonant Inverter for Induction Heating", *Industry Applications Society Annual Meeting*, vol. 2, 1993, pp. 843-849.

[8] Satoshi Nagai, Hirokazu Nagura, Mutsuo Nakaoka, Atsushi Okuno, "High-Frequency Inverter with Phase-Shifted PWM and Load-Adaptive PFM Control Strategy for Industrial Induction-Heating", *Industry Applications Society Annual Meeting*, vol. 3, 1993, pp. 2165-2172.

[9] Jinfei Shen, Hongbin Ma,Wenxu Yan, Jing Hui, Lei Wu, "PDM and PSM Hybrid Power Control of a Series-Resonant Inverter for Induction Heating Applications", *IEEE Conference on Industrial Electronics and Applications*, ICIEA 2006.

[10] J. M. Burdio, L. A. Barragan, F. Monterde, D. Navarro, J. Acero, "Asymmetrical voltage cancellation control for full-bridge series resonant inverters," *IEEE Trans. Power Electronics*, vol. 19, no. 2, 2004, pp. 461-469.

[11] Hector Sarnago, Oscar Lucia, Arturo Mediano, J.M. Burdio, "Class D / DE Dual-Mode-Operation Resonant Converter for Improved-Efficiency Domestic Induction Heating System," *IEEE Transactions on Power Electronics*, vol. 28, no. 3, March 2013, pp. 1274-1285.

[12] F. Forest, E. Laboure, F. Costa, J.Y. Gaspard, "Principle of a multi-load / single converter system for low power induction heating," *IEEE Trans. Power Electronics*, vol.15, no. 2, 2000, pp. 223-230.

[13] Jose M. Burdio, Fernando Monterde, Jose R. Garcia, Luis A. Barragan, Abelardo Martinez, "A Two-Output Series-Resonant Inverter for Induction-Heating Cooking Appliances," *IEEE Trans. Power Electronics*, vol. 20, no. 4, 2005, pp. 815-822.

[14] S. Zenitani, M. Okamoto, E. Hiraki, T. Tanaka, "A Charge Boost Type Multi Output Full-Bridge High Frequency Soft Switching Inverter for IH Cooking Appliance," *14th International Power Electronics and Motion Control Conference* (EPE-PEMC), 2010, pp. T2-127-T2-133.

[15] Oscar Lucia, J.M. Burdio, I. Millan, J. Acero, D. Puyal, "Load-Adaptive Control Algorithm of Half-Bridge Series Resonant Inverter for Domestic Induction Heating," *IEEE Transactions on Industrial Electronics*, vol. 56, no. 8, August 2009, pp. 3106-3116.

[16] Oscar Lucia, Jose M. Burdio, Luis A. Barragan, Claudio Carretero, Jesus Acero, "Series Resonant Multi-inverter with Discontinuous-Mode Control for Improved Light-Load Operation," *IEEE Transactions on Industrial Electronics*, vol. 58, no. 11, November 2011, pp. 5163-5171.

[17] Oscar Lucia, I. Urriza, Luis A. Barragan, D. Navarro, Oscar Jimenez, J.M.Burdio, "Real Time FPGA-Based Hardware-in-the-Loop Simulation Test Bench Applied to Multiple-Output Power Converters," *IEEE Transactions on Industry Applications*, vol. 47, no. 2, March /April 2011, pp. 853-860.

[18] Oscar Lucia, Claudio Carretero, J.M. Burdio, Jesus Acero, and Fernando Almazan, "Multiple-Output Resonant Matrix Converter for Multiple Induction Heaters," *IEEE Transactions on Industry Applications*, vol.48, no. 4, July/August 2012, pp. 1387-1396.

P. Sharath Kumar He received B.Tech degree in Electrical and Electronics Engineering from Jawaharlal Nehru Technological University, Hyderabad, India in 2006 and M.Tech degree from National Institute of Technology, Kurukshetra, India in 2008. Presently pursuing Ph.D in Electrical Engineering at National Institute of Technology, Warangal, India. His area of interest is high frequency resonant inverters.

N. Vishwanathan He received B.Sc (Engg.) degree in electrical engineering from Dayalbagh Educational Institute, Agra, India, in 1990, M.Tech. degree in electrical machines and industrial drives from REC, Warangal, India in 1992, and Ph.D. from Indian Institute of Science, Bangalore, India, in 2004. He is currently working as Professor in the Dept. of Electrical Engg, NIT, Warangal, India. His areas of interest are switched mode power conversion and induction heating applications.

Bhagwan K. Murthy He obtained his B.E. (Electrical) and M.E. (Industrial Electronics) degrees from the M. S. University of Baroda, India in 1983 and 1987, respectively. He did his PhD at IIT Madras in 1999. He is working as Professor of Electrical Engineering in the National Institute of Technology, Warangal, India. His research interests include application of power electronics to DSP controlled industrial drives and renewable energy.